

# Symbol Error Rate of Space-Time Network Coding in Nakagami- $m$ Fading

Ang Yang, Zesong Fei, Nan Yang, Chengwen Xing, and Jingming Kuang

## Abstract

In this paper, we analyze the symbol error rate (SER) of space-time network coding (STNC) in a distributed cooperative network over independent but not necessarily identically distributed (i.n.i.d.) Nakagami- $m$  fading channels. In this network, multiple sources communicate with a single destination with the assistance of multiple decode-and-forward (DF) relays. We first derive new exact closed-form expressions for the SER with  $M$ -ary phase shift-keying modulation ( $M$ -PSK) and  $M$ -ary quadrature amplitude modulation ( $M$ -QAM). We then derive new compact expressions for the asymptotic SER to offer valuable insights into the network behavior in the high signal-to-noise ratio (SNR) regime. Importantly, we demonstrate that STNC guarantees full diversity order, which is determined by the Nakagami- $m$  fading parameters of all the channels but independent of the number of sources. Based on the new expressions, we examine the impact of the number of relays, relay location, Nakagami- $m$  fading parameters, power allocation, and nonorthogonal codes on the SER.

## Index Terms

Space-time network coding, symbol error rate, Nakagami- $m$  fading.

A. Yang, Z. Fei, C. Xing, and J. Kuang are with the School of Information and Electronics, Beijing Institute of Technology, Beijing, China (email: taylorkingyang@163.com, feizesong@bit.edu.cn, chengwenxing@ieee.org, JMKuang@bit.edu.cn).

N. Yang is with the Wireless and Networking Technologies Laboratory, CSIRO ICT Centre, Marsfield, NSW 2122, Australia (email: jonas.yang@csiro.au).

## I. INTRODUCTION

Cooperative communication has been recognized as a promising low-cost solution to combat fading and to extend coverage in wireless networks [1, 2]. The key idea behind this solution is to employ relays to receive and transmit the source information to the destination, which generates a virtual multiple-input and multiple-output (MIMO) system to provide spatial cooperative diversity [3, 4]. Apart from diversity, throughput enhancement is another critical challenge for wireless networks. Against this background, network coding (NC) is proposed as a potentially powerful tool to enable efficient information transmission, where data flows coming from multiple sources are combined to increase throughput [5–7].

Recently, the joint exploitation of cooperative diversity and NC has become a primary design concern in distributed networks with multiple users and multiple relays [8–11]. Motivated by this, [8] investigated various sink network decoding approaches for the network with intermediate node encoding. In [9], linear network coding (LNC) was applied in distributed uplink networks to facilitate the transmission of independent information from multiple users to a common base station. In [10], low-density parity-check (LDPC) code and NC was jointly designed for a multi-source single-relay FDMA system over uniform phase-fading Gaussian channels. In [11], cooperative network coding strategies were proposed for a relay-aided two-source two-destination wireless network with a backhaul connection between the sources.

In order to increase the capacity and transmission reliability of wireless cooperative networks, multiple antennas are deployed to gain the merits of MIMO processing techniques [12–17]. In this strategy, distributed space-time coding (DSTC) was proposed to further boost network performance, where the antennas at the distributed relays are utilized as transmit antennas to generate a space-time code for the receiver [18, 19]. A differential DSTC was proposed in [20] to eliminate the requirement of channel information at the relays and the receiver. The combined benefits of maximum-ratio combining (MRC) and DSTC were investigated in [21]. In [22], the impact of DSTC in two-way amplify-and-forward relay channels was characterized.

One of the principal challenges in distributed cooperative networks is to leverage the benefits from both NC and DSTC. A promising solution that addresses this challenge is space-time network

coding (STNC), which was proposed in [23]. Fundamentally, STNC combines the information from different sources at a relay, which involves the concept of NC. Moreover, STNC transmits the combined signals in several time slots using a set of relays, which involves the concept of DSTC. Based on these, STNC achieves spatial diversity with low transmission delay under the impact of imperfect frequency and timing synchronization. We note that in [23], the performance of STNC was evaluated for Rayleigh fading channels, where no closed-form expression was presented.

In this paper, we consider a distributed cooperative network using STNC over independent but not necessarily identically distributed (i.n.i.d.) Nakagami- $m$  fading channels, which generalizes the result in [23]. In this network, multiple sources communicate with a single destination with the assistance of multiple relays. Here, we focus on decode-and-forward (DF) protocol at the relays, which arises from the fact that this protocol has been successfully deployed in practical wireless standards, e.g., 3GPP Long Term Evolution (LTE) and IEEE 802.16j WiMAX [24]. Different from [23], we examine two fundamental questions as follows: “1) *What is the impact of STNC on the symbol error rate (SER) in general Nakagami- $m$  fading channels?*” and “2) *Can we provide closed-form expressions for the SER in Nakagami- $m$  fading to alleviate the burden of Monte Carlo simulations?*” The rationale behind these questions is that Nakagami- $m$  fading covers a wide range of typical fading scenarios in realistic wireless applications via the  $m$  parameter. Notably, Nakagami- $m$  fading encompasses Rayleigh fading ( $m = 1$ ) as a special case [25]. To tackle these questions, we first derive new closed-form expressions for the exact SER, which are valid for multiple phase shift-keying modulation ( $M$ -PSK) and  $M$ -ary quadrature amplitude modulation ( $M$ -QAM). To further provide valuable insights at high signal-to-noise ratios (SNRs), we derive new compact expressions for the asymptotic SER, from which the diversity gain is obtained. Specifically, it is demonstrated that the diversity order is determined by the Nakagami- $m$  fading parameters of all the channels, but independent of the number of sources. Various numerical results are utilized to examine the impact of the number of relays, relay location, Nakagami- $m$  fading parameters, power allocation, and nonorthogonal codes on the SER. Importantly, it is shown that nonorthogonal codes provide higher throughput than orthogonal codes, while guaranteeing full diversity over Nakagami- $m$  fading channels. Our analytical expressions are substantiated via Monte

Carlo simulations.

## II. SYSTEM MODEL

Fig. 1 depicts a distributed cooperative network where  $L$  sources,  $U_1, U_2, \dots, U_L$ , transmit their own information to a common destination  $D$  with the aid of  $Q$  relays,  $R_1, R_2, \dots, R_Q$ . In this network, each node is equipped with a single antenna. We consider a practical and versatile operating scenario where the source-relay, the relay-destination, and the source-destination channels experience i.n.i.d. Nakagami- $m$  fading. As such, we denote the Nakagami- $m$  fading parameter between  $U_l$  and  $R_q$  as  $m_{lq}$ , the Nakagami- $m$  fading parameter between  $R_q$  and  $D$  as  $m_{qd}$ , and the Nakagami- $m$  fading parameter between  $U_l$  and  $D$  as  $m_{ld}$ . We further denote the channel coefficient between  $U_l$  and  $R_q$  as  $h_{lq}$ , the channel coefficient between  $R_q$  and  $D$  as  $h_{qd}$ , and the channel coefficient between  $U_l$  and  $D$  as  $h_{ld}$ , where  $1 \leq l \leq L$  and  $1 \leq q \leq Q$ . Throughout this paper, we define the variances of these channel coefficients as  $h_{\phi\varphi} \sim \mathcal{CN}(0, d_{\phi\varphi}^{-\alpha})$ , where  $\phi \in \{l, q\}$ ,  $\varphi \in \{q, d\}$ , and  $\phi \neq \varphi$ . Here, we incorporate the path loss in the signal propagation such that  $d_{\phi\varphi}$  denotes the distance between  $\phi$  and  $\varphi$  and  $\alpha$  denotes the path loss exponent.

In this network, the STNC transmission between the sources and the destination is divided into two consecutive phases: 1) source transmission phase and 2) relay transmission phase. In the source transmission phase, the sources transmit their symbols in the designated time slots. In this phase, the relays receive a set of overheard symbols from the sources. In the relay transmission phase, each relay encodes the set of overheard symbols to a single signal and then transmits it to the destination in its designated time slot. As illustrated in Fig. 2,  $(L + Q)$  time slots are required to complete the STNC transmission to eliminate the detrimental effects of imperfect synchronization on any point-to-point transmission in this network at any time slot.

We proceed to detail the transmission in the two phases, as follows:

In the source transmission phase, the signals received at the destination from  $U_l$  in the time slot  $l$  is given by

$$y_{ld}(t) = h_{ld}\sqrt{P_l}x_l s_l(t) + w_{ld}(t), \quad (1)$$

where  $P_l$  denotes the transmit power at  $U_l$ ,  $x_l$  denotes the symbol transmitted by  $U_l$ ,  $s_l(t)$  denotes the

spreading code of  $x_l$ , and  $w_{ld}$  is the additive white Gaussian noise (AWGN) with zero mean and the variance of  $N_0$ . The cross correlation between  $s_p(t)$  and  $s_q(t)$  are expressed as  $\rho_{pq} = \langle s_p(t), s_q(t) \rangle$ , where  $\langle f(t), g(t) \rangle \triangleq \frac{1}{T} \int_0^T f(t) g^*(t) dt$  is the inner product between  $f(t)$  and  $g(t)$  during the symbol interval  $T$ . Moreover, we assume that  $\rho_{ll} = \|s_l(t)\|^2 = 1$ . The signals received at  $R_q$  from  $U_l$  is given by

$$y_{lq}(t) = h_{lq} \sqrt{P_l} x_l s_l(t) + w_{lq}(t), \quad (2)$$

where  $w_{lq}(t)$  is AWGN with zero mean and the variance of  $N_0$ .

In the relay transmission phase, the signal received at the destination from  $R_q$  is given by

$$y_{qd}(t) = h_{qd} \underbrace{\sum_{l=1}^L \beta_{ql} \sqrt{P_{ql}} x_l s_l(t)}_{f_q(x)} + w_{qd}(t), \quad (3)$$

where  $P_{ql}$  denotes the transmit power at  $R_q$  and  $w_{qd}$  is AWGN with zero mean and the variance of  $N_0$ . In (3), the scalar  $\beta_{ql}$  denotes the state whether  $R_q$  decodes  $x_l$  correctly. Specifically,  $\beta_{ql}$  is equal to 1 if  $R_q$  decodes  $x_l$  correctly, but 0 otherwise.

For the detection of the received signals at the destination, we assume that the full knowledge of the channel state information are available at the receivers with the aid of a preamble in the transmitted signal. We also assume that the destination has the detection states at the relays, which can be obtained via an indicator in the relaying signal. At the destination, the spreading codes  $s_l$  is employed such that the information symbols  $x_l$  is separated from  $y_{ld}$  and  $y_{qd}$ , where  $l \in \{1, \dots, L\}$ . For any desired symbol  $x_l$ , the destination combines the information of  $x_l$  from  $U_l$  and the  $Q$  relays using maximum ratio combining (MRC). Therefore, the instantaneous signal-to-noise ratio (SNR) of  $x_l$  is expressed as [23]

$$\gamma_l = \frac{P_l |h_{ld}|^2}{N_0} + \sum_{q=1}^Q \frac{\beta_{ql} P_{lq} |h_{qd}|^2}{N_0 \varepsilon_l}, \quad (4)$$

where  $\varepsilon_l$  is the  $l$ th diagonal element of matrix  $\mathbf{R}^{-1}$  associated with symbol  $x_l$  and  $\mathbf{R}$  is given by

$$\mathbf{R} = \begin{bmatrix} 1 & \rho_{21} & \cdots & \rho_{Q1} \\ \rho_{12} & 1 & \cdots & \rho_{Q2} \\ \vdots & \vdots & \ddots & \vdots \\ \rho_{1Q} & \rho_{2Q} & \cdots & 1 \end{bmatrix}. \quad (5)$$

To facilitate the performance analysis in the following section, we re-express (4) as a unitary expression given by

$$\gamma_l = c_0 |h_0|^2 + \sum_{q=1}^Q \beta_{ql} c_q |h_q|^2, \quad (6)$$

where  $c_0 = P_l d_{dl}^{-\alpha} / N_0$  denotes the equivalent SNR at  $D$  received from  $U_l$ ,  $h_0$  denotes the unitary Nakagami- $m$  fading coefficient between  $U_l$  and  $D$  with variance one,  $c_q = P_l d_{ql}^{-\alpha} / N_0 \varepsilon_l$  denotes the  $q$ th equivalent SNR received at  $D$  from  $R_q$ , and  $h_q$  denotes the unitary Nakagami- $m$  fading coefficient between  $R_q$  and  $D$  with variance one.

### III. SER ANALYSIS OVER NAKAGAMI- $m$ FADING CHANNEL

In this section, we first derive new closed-form expressions for the exact SER with  $M$ -PSK and  $M$ -QAM. We then derive new compact expressions for the asymptotic SER, which will allow us to examine the network behavior in the high SNR regime.

#### A. Exact SER

In DF protocol,  $\beta_{ql}$  denotes the decoding state at  $R_q$  associated with  $x_l$ . Based on the values of all  $\beta_{ql}$ 's, we define a decimal number as  $S_l = [\beta_{1l} \beta_{2l} \cdots \beta_{Ql}]_2$  to represent one of  $2^Q$  network decoding states at  $Q$  relays associated with  $x_l$ . Since all the channels in this network are mutually independent, the events that whether  $R_q$  correctly decodes the received signal are independent. It follows that  $\beta_{ql}$ 's are independent Bernoulli random variables, the distribution of which is written as

$$G(\beta_{ql}) = \begin{cases} 1 - \text{SER}_{ql}, & \text{if } \beta_{ql} = 1 \\ \text{SER}_{ql}, & \text{otherwise,} \end{cases} \quad (7)$$

where  $\text{SER}_{ql}$  denotes the SER of detecting  $x_l$  at  $R_q$ . Therefore, the joint probability of a particular combination of  $x_l$  in  $S_l$  is written as

$$\Pr(S_l) = \prod_{q=1}^Q G(\beta_{ql}). \quad (8)$$

Applying Bayesian rule, the SER of detecting  $x_l$  at  $D$  is derived as

$$\text{SER}_l = \sum_{S_l=0}^{2^Q-1} \text{SER}_{\gamma_l|S_l} \Pr(S_l) = \sum_{S_l=0}^{2^Q-1} \text{SER}_{\gamma_l|S_l} \prod_{q=1}^Q G(\beta_{ql}), \quad (9)$$

where  $\text{SER}_{\gamma_{l|S_l}}$  denotes the SER of detecting  $x_l$  at  $D$  conditioned on  $S_l$ . To facilitate the calculation of (9), we present the exact closed-form results for  $\text{SER}_{\gamma_{l|S_l}}$  and  $G(\beta_{ql})$ , as follows.

1) *Exact Results for  $\text{SER}_{\gamma_{l|S_l}}$* : We commence the derivation of  $\text{SER}_{\gamma_{l|S_l}}$  by presenting the PDF of  $\gamma_{l|S_l}$ ,  $f_{\gamma_{l|S_l}}(v)$ . If there are  $N$  “1” elements in one set  $S_l$ , let  $a_1, a_2, \dots, a_N \in \{c_1, c_2, \dots, c_Q\}$  denote the equivalent SNRs of the  $N$  relays which decode  $x_l$  successfully, where  $N \leq Q$ . We then define  $a_0 = c_0$  to make the source equivalent to the zeroth relay. As such, the SNR at  $D$  to one desired symbol  $x_l$  can be rewritten as

$$\gamma_{l|S_l} = a_0 |h_0|^2 + \sum_{n=1}^N a_n |h_n|^2 = \sum_{n=0}^N \underbrace{a_n |h_n|^2}_{Y_n}. \quad (10)$$

According to [25], the PDF of  $Y_n$  in Nakagami- $m$  fading is given by

$$f_{Y_n}(y) = \frac{m_n^{m_n} y^{m_n-1}}{a_n^{m_n} \Gamma(m_n)} \exp\left(-\frac{m_n y}{a_n}\right), \quad (11)$$

where  $m_n$  is the Nakagami- $m$  fading parameter between the  $n$ th successful relay and the destination. For example, if the first and the second relays out of three relays successfully decode the information from  $U_l$ , we have  $m_1 = m_{1d}$  and  $m_2 = m_{2d}$ . Using Fourier transform together with [26, eq. (3.351.3)], the characteristic function (CF) of  $Y_n$  is calculated as

$$C_{Y_n}(u) = \int_{-\infty}^{\infty} f_{Y_n}(y) e^{juy} dy = \left(1 - \frac{jua_n}{m_n}\right)^{-m_n}. \quad (12)$$

Given that  $\gamma_{l|S_l}$  is the sum of  $Y_n$ 's, the CF of  $\gamma_{l|S_l}$  is obtained as

$$C_{\gamma_{l|S_l}}(u) = \prod_{n=0}^N C_{Y_n}(u) = \prod_{n=0}^N \left(1 - \frac{jua_n}{m_n}\right)^{-m_n}. \quad (13)$$

Applying inverse Fourier transform, the PDF of  $\gamma_{l|S_l}$  is derived as

$$\begin{aligned} f_{\gamma_{l|S_l}}(v) &= \frac{1}{2\pi} \int_{-\infty}^{\infty} C_{\gamma_{l|S_l}}(u) e^{-juv} du \\ &= \frac{1}{2\pi} \int_{-\infty}^{\infty} \underbrace{\left( \prod_{n=0}^N \left(1 - \frac{jua_n}{m_n}\right)^{-m_n} \right)}_{g(u)} e^{-juv} du. \end{aligned} \quad (14)$$

We next seek the solution for  $g(u)$ . Due to the randomness of the wireless channels, we note that  $g(u)$  has  $N + 1$  different poles  $z_0 = -jm_0/a_0$ ,  $z_1 = -jm_1/a_1$ ,  $\dots$ ,  $z_N = -jm_N/a_N$  in complex

field. As such, based on residue theorem [27], the residue of  $k^{\text{th}}$  pole of  $g(u)$  in complex field can be expressed as

$$\begin{aligned} \text{Res}[g(z_k), z_k] &= \frac{1}{(m_k - 1)!} \lim_{u \rightarrow z_k} \frac{d^{m_k-1}}{du^{m_k-1}} [(u - z_k)^{m_k} g(u)] \\ &= \frac{m_k^{m_k}}{(-j)^{m_k} a_k^{m_k} (m_k - 1)!} \lim_{u \rightarrow z_k} \frac{d^{m_k-1}}{du^{m_k-1}} \left[ e^{-juv} \left( \prod_{n=0, n \neq k}^N \left( 1 - \frac{jua_n}{m_n} \right)^{-m_n} \right) \right]. \end{aligned} \quad (15)$$

As per the general Leibniz's rule, we derive  $\text{Res}[g(z_k), z_k]$  in (15) as

$$\begin{aligned} &\text{Res}[g(z_k), z_k] \\ &= \frac{m_k^{m_k}}{(-j)^{m_k} a_k^{m_k} (m_k - 1)!} \lim_{u \rightarrow z_k} \sum_{i=0}^{m_k-1} \left[ (-jv)^{m_k-1-i} e^{-juv} \right] \sum_{i_0=0}^i \sum_{i_1=0}^{i_0} \cdots \sum_{i_{k-1}=0}^{i_{k-2}} \sum_{i_{k+1}=0}^{i_{k-1}} \cdots \sum_{i_{N-1}=0}^{i_{N-2}} \\ &\quad \times \binom{m_k-1}{i} \binom{i}{i_0} \binom{i_0}{i_1} \cdots \binom{i_{k-2}}{i_{k-1}} \binom{i_{k-1}}{i_{k+1}} \cdots \binom{i_{N-2}}{i_{N-1}} \left[ \frac{d^{i_{N-1}}}{du^{i_{N-1}}} \left( 1 - \frac{jua_N}{m_N} \right)^{-m_N} \right] \\ &\quad \times \left[ \frac{d^{i_{N-2}-i_{N-1}}}{du^{i_{N-2}-i_{N-1}}} \left( 1 - \frac{jua_{N-1}}{m_{N-1}} \right)^{-m_{N-1}} \right] \cdots \left[ \frac{d^{i_{k-1}-i_{k+1}}}{du^{i_{k-1}-i_{k+1}}} \left( 1 - \frac{jua_{k+1}}{m_{k+1}} \right)^{-m_{k+1}} \right] \\ &\quad \times \left[ \frac{d^{i_{k-2}-i_{k-1}}}{du^{i_{k-2}-i_{k-1}}} \left( 1 - \frac{jua_{k-1}}{m_{k-1}} \right)^{-m_{k-1}} \right] \cdots \left[ \frac{d^{i_0-i_1}}{du^{i_0-i_1}} \left( 1 - \frac{jua_1}{m_1} \right)^{-m_1} \right] \left[ \frac{d^{i-i_0}}{du^{i-i_0}} \left( 1 - \frac{jua_0}{m_0} \right)^{-m_0} \right]. \end{aligned} \quad (16)$$

Upon close observation, we simplify (16) as

$$\text{Res}[g(z_k), z_k] = \sum_{i=0}^{m_k-1} j B_{N,k,i} v^{m_k-1-i} \exp\left(-\frac{m_k v}{a_k}\right), \quad (17)$$

where  $B_{N,k,i}$  is defined as

$$\begin{aligned} &B_{N,k,i} \quad (18) \\ &= \frac{m_k^{m_k} (-1)^{-i}}{a_k^{m_k} (m_k - 1)!} \sum_{i_0=0}^i \sum_{i_1=0}^{i_0} \cdots \sum_{i_{k-1}=0}^{i_{k-2}} \sum_{i_{k+1}=0}^{i_{k-1}} \cdots \sum_{i_{N-1}=0}^{i_{N-2}} \binom{m_k-1}{i} \binom{i}{i_0} \binom{i_0}{i_1} \cdots \binom{i_{k-2}}{i_{k-1}} \binom{i_{k-1}}{i_{k+1}} \cdots \binom{i_{N-2}}{i_{N-1}} \\ &\quad \times \left( \frac{a_N}{m_N} \right)^{i_{N-1}} \left( \frac{a_{N-1}}{m_{N-1}} \right)^{i_{N-2}-i_{N-1}} \cdots \left( \frac{a_{k+1}}{m_{k+1}} \right)^{i_{k-1}-i_{k+1}} \left( \frac{a_{k-1}}{m_{k-1}} \right)^{i_{k-2}-i_{k+1}} \cdots \left( \frac{a_1}{m_1} \right)^{i_0-i_1} \left( \frac{a_0}{m_0} \right)^{i-i_0} \\ &\quad \times (m_N)_{i_{N-1}} (m_{N-1})_{i_{N-2}-i_{N-1}} \cdots (m_{k+1})_{i_{k-1}-i_{k+1}} (m_{k-1})_{i_{k-2}-i_{k-1}} \cdots (m_1)_{i_0-i_1} (m_0)_{i-i_0} \\ &\quad \times \left( 1 - \frac{m_k a_N}{m_N a_k} \right)^{-m_N-i_{N-1}} \left( 1 - \frac{m_k a_{N-1}}{m_{N-1} a_k} \right)^{-m_{N-1}-i_{N-2}+i_{N-1}} \cdots \left( 1 - \frac{m_k a_{k+1}}{m_{k+1} a_k} \right)^{-m_{k+1}-i_{k-1}+i_{k+1}} \\ &\quad \times \left( 1 - \frac{m_k a_{k-1}}{m_{k-1} a_k} \right)^{-m_{k-1}-i_{k-2}+i_{k-1}} \cdots \left( 1 - \frac{m_k a_1}{m_1 a_k} \right)^{-m_1-i_0+i_1} \left( 1 - \frac{m_k a_0}{m_0 a_k} \right)^{-m_0-i+i_0}, \end{aligned} \quad (19)$$



and  $(m_n)_i = \Gamma(m_n + i) / \Gamma(m_n)$  is the Pochmann symbol. Based on the residues of the poles, we confirm that  $g(u)$  is available for the residue theorem. Specifically, using the residue of  $k^{\text{th}}$  pole of  $g(u)$  in complex field, we obtain

$$\int_{-\infty}^{\infty} g(u) du = -2\pi j \sum_{k=0}^N \text{Res}[g(z_k), z_k]. \quad (20)$$

The proof of (20) is shown in Appendix A. Based on (17) and (20), the PDF of  $\gamma_{|S_l}$  in (14) is derived as

$$f_{\gamma_{|S_l}}(v) = \sum_{k=0}^N \sum_{i=0}^{m_k-1} B_{N,k,i} v^{m_k-1-i} \exp\left(-\frac{m_k v}{a_k}\right). \quad (21)$$

With the aid of  $f_{\gamma_{|S_l}}(v)$  in (21), we are capable to derive  $\text{SER}_{\gamma_{|S_l}}$  for  $M$ -PSK and  $M$ -QAM.

First,  $\text{SER}_{\gamma_{|S_l}}$  for  $M$ -PSK is derived as

$$\begin{aligned} \text{SER}_{\gamma_{|S_l}, \text{MPSK}} &= \frac{1}{\pi} \int_0^{(M-1)\pi/M} \int_0^{\infty} \alpha \exp\left(-\frac{b\gamma}{\sin^2\theta}\right) f_{\gamma_{|S_l}}(\gamma) d\gamma d\theta \\ &= \frac{\alpha}{\pi} \sum_{k=0}^N \sum_{i=0}^{m_k-1} B_{N,k,i} \int_0^{(M-1)\pi/M} \int_0^{\infty} \gamma^{m_k-1-i} \exp\left(\left(-\frac{b}{\sin^2\theta} - \frac{m_k}{a_k}\right)\gamma\right) d\gamma d\theta, \end{aligned} \quad (22)$$

where  $\alpha$  and  $b$  are modulation specific constants. For  $M$ -PSK,  $\alpha = 1$  and  $b = \sin^2(\pi/M)$ . With the aid of [26, eq. (3.351.3)] and [28, eq. (5A.17)], (22) is derived as

$$\begin{aligned} &\text{SER}_{\gamma_{|S_l}, \text{MPSK}} \\ &= \frac{\alpha}{\pi} \sum_{k=0}^N \sum_{i=0}^{m_k-1} B_{N,k,i} \Gamma(m_k - i) \int_0^{(M-1)\pi/M} \left(\frac{b}{\sin^2\theta} + \frac{m_k}{a_k}\right)^{-m_k+i} d\theta \\ &= \alpha \sum_{k=0}^N \sum_{i=0}^{m_k-1} B_{N,k,i} \Gamma(m_k - i) \left(\frac{a_k}{m_k}\right)^{m_k-i} \left[ \frac{M-1}{M} - \frac{1}{\pi} \sqrt{\frac{a_k b}{a_k b + m_k}} \left( \left(\frac{\pi}{2} + \tan^{-1}\omega\right) \sum_{p=0}^{m_k-i-1} \binom{2p}{p} \right. \right. \\ &\quad \left. \left. \times \left(4 \left(1 + \frac{a_k b}{m_k}\right)\right)^{-p} + \sin(\tan^{-1}\omega) \sum_{p=1}^{m_k-i-1} \sum_{t=1}^p T_{p,t} \left(1 + \frac{a_k b}{m_k}\right)^{-p} (\cos(\tan^{-1}\omega))^{2(p-t)+1} \right) \right], \end{aligned} \quad (23)$$

where  $\omega = \sqrt{\frac{a_k b}{a_k b + m_k}} \cot \frac{\pi}{M}$  and  $T_{p,t} = \frac{\binom{2p}{p}}{\binom{2(p-t)}{p-t} 4^t [2(p-t)+1]}$ .

We then derive  $\text{SER}_{\gamma_{|S_l}}$  for  $M$ -QAM as

$$\begin{aligned} \text{SER}_{\gamma_{|S_l}, \text{MQAM}} &= \frac{4}{\pi} \int_0^{\pi/2} \int_0^{\infty} \alpha \exp\left(-\frac{b\gamma}{\sin^2\theta}\right) f_{\gamma_{|S_l}}(\gamma) d\gamma d\theta \\ &\quad - \frac{4}{\pi} \int_0^{\pi/4} \int_0^{\infty} \alpha^2 \exp\left(-\frac{b\gamma}{\sin^2\theta}\right) f_{\gamma_{|S_l}}(\gamma) d\gamma d\theta, \end{aligned} \quad (24)$$

where  $\alpha = 4 \left(1 - 1/\sqrt{M}\right)$  and  $b = 3/(2(M-1))$ . Calculating the integrals in (24),  $\text{SER}_{\gamma_{l|S_l}, \text{MQAM}}$  is derived as

$$\begin{aligned}
& \text{SER}_{\gamma_{l|S_l}, \text{MQAM}} \\
&= 4\alpha \sum_{k=0}^N \sum_{i=0}^{m_k-1} B_{k,i} \Gamma(m_k - i) \left(\frac{a_k}{m_k}\right)^{m_i-i} \left[ \frac{1}{2} - \frac{1}{\pi} \sqrt{\frac{a_k b}{a_k b + m_k}} \left( \left(\frac{\pi}{2} + \tan^{-1} \omega_1\right) \sum_{p=0}^{m_k-i-1} \binom{2p}{p} \right. \right. \\
& \quad \left. \left. \times \left(4 \left(1 + \frac{a_k b}{m_k}\right)\right)^{-p} + \sin(\tan^{-1} \omega_1) \sum_{p=1}^{m_i-1} \sum_{q=1}^p T_{p,q} \left(1 + \frac{a_k b}{m_k}\right)^{-p} (\cos(\tan^{-1} \omega_1))^{2(p-q)+1} \right) \right] \\
& - 4\alpha^2 \sum_{k=0}^N \sum_{i=0}^{m_k-1} B_{k,i} \Gamma(m_k - i) \left(\frac{a_k}{m_k}\right)^{m_i-i} \left[ \frac{1}{4} - \frac{1}{\pi} \sqrt{\frac{a_k b}{a_k b + m_k}} \left( \left(\frac{\pi}{2} - \tan^{-1} \omega_2\right) \sum_{p=0}^{m_k-i-1} \binom{2p}{p} \right. \right. \\
& \quad \left. \left. \times \left(4 \left(1 + \frac{a_k b}{m_k}\right)\right)^{-p} - \sin(\tan^{-1} \omega_2) \sum_{p=1}^{m_i-1} \sum_{q=1}^p T_{p,q} \left(1 + \frac{a_k b}{m_k}\right)^{-p} (\cos(\tan^{-1} \omega_2))^{2(p-q)+1} \right) \right], \tag{25}
\end{aligned}$$

where  $\omega_1 = \sqrt{\frac{a_k b}{a_k b + m_k}} \cot \frac{\pi}{2}$  and  $\omega_2 = \sqrt{\frac{a_k b}{a_k b + m_k}} \cot \frac{\pi}{4}$ .

2) *Exact Results for  $G(\beta_{ql})$* : We now analyze  $G(\beta_{ql})$  for  $M$ -PSK and  $M$ -QAM, respectively. According to (7), it is equivalent to analyze  $\text{SER}_{ql}$ . Using (2), the received SNR at  $R_q$  is written as

$$\gamma_{ql} = \frac{P_l |h_{ql}|^2}{N_0} = \frac{P_l d_{ql}^{-\alpha}}{N_0} |h|^2 = c_{ql} |h|^2, \tag{26}$$

where  $c_{ql} = P_l d_{ql}^{-\alpha}/N_0$  denotes the equivalent SNR at  $R_q$  received from  $U_l$ , and  $h$  denotes the unitary Nakagami- $m$  fading coefficients between  $U_l$  and  $R_q$  with variance one.

We first derive  $\text{SER}_{ql}$  for  $M$ -PSK as

$$\begin{aligned}
\text{SER}_{ql, \text{MPSK}} &= \frac{\alpha(M-1)}{M} - \frac{\alpha}{\pi} \sqrt{\frac{c_{ql} b}{c_{ql} b + m_{lq}}} \left[ \left(\frac{\pi}{2} + \tan^{-1} \varpi\right) \sum_{p=0}^{m_{lq}-1} \binom{2p}{p} \left(4 \left(1 + \frac{c_{ql} b}{m_{lq}}\right)\right)^{-p} \right. \\
& \quad \left. + \sin(\tan^{-1} \varpi) \sum_{p=1}^{m_{lq}-1} \sum_{t=1}^p T_{p,t} \left(1 + \frac{c_{ql} b}{m_{lq}}\right)^{-p} (\cos(\tan^{-1} \varpi))^{2(p-t)+1} \right], \tag{27}
\end{aligned}$$

where  $\varpi = \sqrt{\frac{c_{ql} b}{c_{ql} b + m_{lq}}} \cot \frac{\pi}{M}$ .

We then derive  $\text{SER}_{q_l}$  for  $M$ -QAM as

$$\begin{aligned} \text{SER}_{q_l, \text{MQAM}} = & 2\alpha - \frac{4\alpha}{\pi} \sqrt{\frac{c_{q_l} b}{c_{q_l} b + m_k}} \left[ \left( \frac{\pi}{2} + \tan^{-1} \varpi_1 \right) \sum_{p=0}^{m_k-i-1} \binom{2p}{p} \left( 4 \left( 1 + \frac{c_{q_l} b}{m_k} \right) \right)^{-p} \right. \\ & \left. + \sin(\tan^{-1} \varpi_1) \sum_{p=1}^{m-i-1} \sum_{q=1}^p T_{p,q} \left( 1 + \frac{c_{q_l} b}{m_k} \right)^{-p} (\cos(\tan^{-1} \varpi_1))^{2(p-q)+1} \right] \\ & - \alpha^2 + \frac{4\alpha^2}{\pi} \sqrt{\frac{a_k b}{a_k b + m_k}} \left[ \left( \frac{\pi}{2} - \tan^{-1} \varpi_2 \right) \sum_{p=0}^{m_k-i-1} \binom{2p}{p} \left( 4 \left( 1 + \frac{c_{q_l} b}{m_k} \right) \right)^{-p} \right. \\ & \left. - \sin(\tan^{-1} \varpi_2) \sum_{p=1}^{m-i-1} \sum_{q=1}^p T_{p,q} \left( 1 + \frac{c_{q_l} b}{m_k} \right)^{-p} (\cos(\tan^{-1} \varpi_2))^{2(p-q)+1} \right], \quad (28) \end{aligned}$$

where  $\varpi_1 = \sqrt{\frac{c_{q_l} b}{a_k b + m_{l_q}}} \cot \frac{\pi}{2}$  and  $\varpi_2 = \sqrt{\frac{c_{q_l} b}{a_k b + m_{l_q}}} \cot \frac{\pi}{4}$ .

Substituting (27) and (28) into (7), we obtain  $G(\beta_{q_l})$  for  $M$ -PSK and  $M$ -QAM, respectively. Therefore, we insert (7) and (23) into (9), which yields the exact closed-form SER for  $M$ -PSK, and substitute (7) and (25) into (9), which gives the exact SER for  $M$ -QAM. Observing (23), (25), (27), and (28), we see that the exact SER expressions for  $M$ -PSK and  $M$ -QAM are given in closed-form and are valid to arbitrary numbers of sources and relays.

## B. Asymptotic SER

We now provide useful insights into the network behavior in the high SNR regime. In doing so, new compact closed-form expressions are presented for the asymptotic SER.

We first focus on  $M$ -PSK. Based on (10),  $\text{SER}_{\gamma_{l|S_l}}$  for  $M$ -PSK can be alternatively written as

$$\begin{aligned} \text{SER}_{\gamma_{l|S_l}, \text{MPSK}} &= \frac{\alpha}{\pi} \int_0^{(M-1)\pi/M} \int_0^\infty \exp\left(-\frac{b\gamma_{l|S_l}}{\sin^2 \theta}\right) f_{\gamma_{l|S_l}}(\gamma_{l|S_l}) d\gamma_{l|S_l} d\theta \\ &= \frac{\alpha}{\pi} \int_0^{(M-1)\pi/M} \left( \int_0^\infty \int_0^\infty \cdots \int_0^\infty \exp\left(-\frac{b \sum_{i=0}^N y_i}{\sin^2 \theta}\right) \left( \prod_{i=0}^N f_{Y_i}(y_i) \right) \prod_{i=0}^N dy_i \right) d\theta. \quad (29) \end{aligned}$$

Substituting (11) into (29) and using [26, eq. (3.351.3)], we obtain  $\text{SER}_{\gamma_{l|S_l}, \text{MPSK}}$  as

$$\begin{aligned} \text{SER}_{\gamma_{l|S_l}, \text{MPSK}} &= \frac{\alpha}{\pi} \int_0^{(M-1)\pi/M} \prod_{i=0}^N \left( \int_0^\infty \frac{m_i^{m_i} y_i^{m_i-1}}{a_i^{m_i} \Gamma(m_i)} \exp\left(-\left(\frac{b}{\sin^2 \theta} + \frac{m_i}{a_i}\right) y_i\right) dy_i \right) d\theta \\ &= \frac{\alpha}{\pi} \int_0^{(M-1)\pi/M} \prod_{i=0}^N \left( \frac{m_i^{m_i}}{a_i^{m_i}} \left( \frac{b}{\sin^2 \theta} + \frac{m_i}{a_i} \right)^{-m_i} \right) d\theta. \quad (30) \end{aligned}$$

We next use [26, eq. (2.513.1)] to develop an asymptotic expression for  $\text{SER}_{\gamma_{l|S_l},\text{MPSK}}$  as

$$\begin{aligned}\text{SER}_{\gamma_{l|S_l},\text{MPSK}}^\infty &\leq \frac{\alpha}{\pi} \int_0^{(M-1)\pi/M} \prod_{i=0}^N \left( \frac{m_i}{a_i} \left( \frac{b}{\sin^2\theta} \right)^{-m_i} \right) d\theta \\ &= \frac{\alpha}{\pi} \left( \prod_{i=0}^N \left( \frac{m_i}{a_i b} \right)^{m_i} \right) \int_0^{(M-1)\pi/M} \sin^{2\sum_{i=0}^N m_i} \theta d\theta \\ &= \frac{\alpha}{\pi b^{\sum_{i=0}^N m_i}} A_{M,N} \prod_{i=0}^N \left( \frac{m_i}{a_i} \right)^{m_i}\end{aligned}\quad (31)$$

where

$$\begin{aligned}A_{M,N} &= \frac{1}{2^{2\sum_{i=0}^N m_i}} \binom{2\sum_{i=0}^N m_i}{\sum_{i=0}^N m_i} \frac{(M-1)\pi}{M} + \frac{(-1)^{\sum_{i=0}^N m_i}}{2^{2\sum_{i=0}^N m_i - 1}} \\ &\quad \times \sum_{k=0}^{\sum_{i=0}^N m_i - 1} (-1)^k \binom{2\sum_{i=0}^N m_i}{k} \frac{\sin\left(\left(2\sum_{i=0}^N m_i - 2k\right) \frac{(M-1)\pi}{M}\right)}{2\sum_{i=0}^N m_i - 2k}.\end{aligned}\quad (32)$$

Similarly, an asymptotic expression for  $\text{SER}_{q_l,\text{MPSK}}$  is obtained as

$$\text{SER}_{q_l,\text{MPSK}}^\infty \leq \frac{\alpha}{\pi} \left( \frac{m_{lq}}{b} \right)^{m_{lq}} \frac{A_{M,m_{lq},0}}{c_{q_l}^{m_{lq}}}.\quad (33)$$

Correspondingly, the asymptotic  $G(\beta_{q_l})$  for  $M$ -PSK is given as

$$G(\beta_{q_l})_{\text{MPSK}}^\infty = \begin{cases} 1, & \text{if } \beta_{q_l} = 1 \\ \text{SER}_{q_l,\text{MPSK}}^\infty, & \text{otherwise.} \end{cases}\quad (34)$$

Based on (31), (33), and (34), the asymptotic SER for  $M$ -PSK is derived as

$$\text{SER}_{l,\text{MPSK}}^\infty = \sum_{S_l=0}^{2^Q-1} \text{SER}_{\gamma_{l|S_l},\text{MPSK}}^\infty \prod_{q=1}^Q G(\beta_{q_l})_{\text{MPSK}}^\infty.\quad (35)$$

Following the same procedure outlined for  $M$ -PSK, we derive the asymptotic SER for  $M$ -QAM as

$$\text{SER}_{l,\text{MQAM}}^\infty = \sum_{S_l=0}^{2^Q-1} \text{SER}_{\gamma_{l|S_l},\text{MQAM}}^\infty \prod_{q=1}^Q G(\beta_{q_l})_{\text{MQAM}}^\infty,\quad (36)$$

where the asymptotic  $\text{SER}_{\gamma_{l|S_l}}$  for  $M$ -QAM is derived as

$$\text{SER}_{\gamma_{l|S_l},\text{MQAM}}^\infty \leq \frac{4\alpha}{\pi b^{\sum_{i=0}^N m_i}} A_{2,N} \prod_{i=0}^N \left( \frac{m_i}{a_i} \right)^{m_i} - \frac{4\alpha^2}{\pi b^{\sum_{i=0}^N m_i}} A_{4/3,N} \prod_{i=0}^N \left( \frac{m_i}{a_i} \right)^{m_i},\quad (37)$$

with  $A_{2,m_i,N}$  and  $A_{4/3,m_i,N}$  being defined in (32), and the asymptotic  $G(\beta_{q_l})$  for  $M$ -QAM is derived

as

$$G(\beta_{q_l})_{\text{MQAM}}^\infty = \begin{cases} 1, & \text{if } \beta_{q_l} = 1 \\ \text{SER}_{q_l,\text{MQAM}}^\infty, & \text{otherwise,} \end{cases}\quad (38)$$

with

$$\text{SER}_{ql,\text{MQAM}}^\infty \leq \frac{4\alpha}{\pi} \left(\frac{m_{lq}}{b}\right)^{m_{lq}} \frac{A_{2,m_{lq},0}}{c_{ql}^{m_{lq}}} - \frac{4\alpha^2}{\pi} \left(\frac{m_{lq}}{b}\right)^{m_{lq}} \frac{A_{4/3,m_{lq},0}}{c_{ql}^{m_{lq}}}. \quad (39)$$

Based on (35) and (36), we next examine the diversity order of the network, which represents the slope of the SER against average SNR in a log-log scale. According to (35) and (36), the asymptotic SER of  $U_l$  can be rewritten as

$$\text{SER}_l^\infty = \sum_{S_l=0}^{2^Q-1} \Theta_{S_l} \left[ \prod_{i=0}^N \frac{1}{a_i^{m_i}} \right] \prod_{q=1}^Q \frac{1}{c_{ql}^{m_{lq}}}, \quad (40)$$

where  $\Theta_{S_l}$  denotes the coefficient independent of  $a_i$  and  $c_{ql}$ , in which the diversity order can be confirmed as

$$\text{div} = m_{ld} + \sum_{q=1}^Q \min(m_{qd}, m_{lq}). \quad (41)$$

It is evident from (41) that the full diversity order is achieved, which is determined by the Nakagami- $m$  fading parameters of all the channels. Notably, the diversity order is independent of the number of sources. In particular, this full diversity order is preserved even non-orthogonal STNC codes are employed.

#### IV. SIMULATION AND NUMERICAL RESULTS

In this section, simulation and numerical results are presented to examine the impact of network parameters with STNC (e.g., the number of relays, the relay location, Nakagami- $m$  fading parameters, and power allocation) on the SER of  $U_l$ . In the figures, we consider a practical scenario where the relays are placed at different distances from  $D$  and  $U_l$  with  $c_j \neq c_i$  and  $c_{jl} \neq c_{il}$  for  $j \neq i$ . We set the distance between  $U_l$  and  $D$  as  $d_{ld} = 1$ . The cross correlations between different spread codes, defined in (1), are set to be zero. We also assume equal transmit power at each node. Further, our results concentrate on the practical example of a highly shadowed area with the path loss exponent as  $\alpha = 3.5$  [29]. In the figures, the exact SER for  $M$ -PSK is evaluated by substituting (7), (23), and (27) into (9), and the exact SER for  $M$ -QAM is evaluated by substituting (7), (25), and (28) into (9). The asymptotic SER for  $M$ -PSK and  $M$ -QAM is calculated from (35) and (36), respectively.

### A. Impact of Number of Relays and Equal Nakagami- $m$ Fading Parameters

In this subsection, we focus on equal Nakagami- $m$  fading parameters with  $m_i = m$ . The average received SNRs are set as  $c_{(i+1)l} = c_{i+1} = c_i + 0.1\gamma_\Delta$  and  $c_0 = c_{0l} = 0.6\gamma_\Delta$ . Fig. 3 plots the exact and asymptotic SER with 4QAM. Fig. 4 plots the exact and asymptotic SER with 8PSK. From Figs. 3 and 4, we see that the asymptotic SER curves accurately predict the exact ones in the high SNR regime. By observing these asymptotic curves, it is evident that the diversity order increases with  $Q$ , which indicates that increasing the number of relays brings an improved performance. It is also seen that the diversity order increases with  $m$ , which indicates that the improvement in fading channels leads to a reduction in the SER. Moreover, we see that the simulation points are in precise agreement with our exact analytical curves, which demonstrates the correctness of our analysis in Section III. Comparing the SER in Fig. 3 with that in Fig. 4, we further see a poorer network performance is achieved by higher order modulation schemes.

### B. Impact of Relay Location

In this subsection, we consider  $d_{lq} \neq d_{qd}$ , which leads to  $c_q \neq c_{qd}$ , and consider equal Nakagami- $m$  fading parameters with  $m_i = m = 2$ . We further normalize  $d_{ld}$  to unity with  $d_{ld} = 1$ . Fig. 5 plots the exact SER with BPSK for  $Q = 2$ . In this figure, *Cases 1, 2, 3* represent the scenario where the relays are located close to the source, while *Cases 4, 5, 6* represent the scenario where the relays are located close to the destination.

We first consider *Cases 1, 2, and 3*. We see that *Case 1* offers a prominent SNR advantage relative to *Case 2*. This indicates that the reduction in the distance between the relay and the destination brings a substantial SER improvement. We also see that *Case 1* and *Case 3* achieve almost the same SER across the entire SNR range. This indicates that the SER improvement from the reduced distance between the source and the relay is negligible. These observations are due to the fact that the network performance is dominant by the relay-destination link when the relays are close to the source. As such, the quality improvement of the relay-destination link has a higher positive impact on the SER than that of the source-relay link.

We next consider *Cases 4, 5, and 6*. It is seen that *Case 4* provides a substantial SNR advantage

compared to *Case 5*. It is also seen that *Case 4* achieves a slight SNR advantage compared to *Case 6*. These observations are explained by the fact that the network performance is dominant by the source-relay link when the relays are close to the destination.

### C. Impact of Unequal Nakagami- $m$ Fading Parameters

We concentrate on unequal Nakagami- $m$  fading parameters and set the average received SNRs as  $c_{(i+1)l} = c_{i+1} = c_i + 0.1\gamma_\Delta$  and  $c_0 = c_{0l} = 0.6\gamma_\Delta$ . Fig. 6 plots the exact SER with 4QAM for  $Q = 2$ . This figure clearly shows that the diversity order in (41) is accurate. For example, it is evident that the asymptotic SER curves of *Cases 1, 2, and 3* are in parallel, which indicates that they achieve the same diversity order. As indicated in (41), *Cases 1, 2, and 3* achieve identical diversity order of 3. Moreover, we see that the diversity order of *Case 4* increases to 4, and the diversity order of *Case 5* increases to 6. This is predicted by (41), which shows that the diversity order is determined by the Nakagami- $m$  fading parameters of all the channels.

### D. Impact of Power Allocation

We now focus on arbitrary transmit power at each node. We consider equal Nakagami- $m$  fading parameters with  $m_i = m = 2$ , set the relay location as  $d_{l1} = 0.8$ ,  $d_{l2} = 1$ ,  $d_{1d} = 0.9$ , and  $d_{2d} = 0.7$ , and normalize  $d_{ld}$  as  $d_{ld} = 1$ . We denote the transmit powers at  $U_l$ ,  $R_1$ , and  $R_2$  as  $P_0$ ,  $P_1$ , and  $P_2$ , respectively. Under the total power constraint, we have  $P_0 + P_1 + P_2 = 3P$ . Fig. 7 plots the exact SER versus  $\xi = P_1/(P_1 + P_2)$  with 4QAM for  $Q = 2$  and  $P/N_0 = 12$  dB. We see that the optimal value of  $P_1/P_2$  depends on  $P_0$ . For example, the optimal power allocation is at  $P_1 = 1.75P$  and  $P_2 = 0.75P$  when  $P_0 = 0.5P$ . Moreover, the optimal power allocation is at  $P_1 = P_2 = 0.5P$  when  $P_0 = 2P$ . Using our SER expressions with different relay locations, iterative search method can be used to find the optimal power allocation that minimizes the SER.

### E. Impact of Nonorthogonal Codes

We now turn our attention to the impact of nonorthogonal codes. We consider  $\rho_{pq} = \rho \neq 0$  for all  $p, q$  and equal Nakagami- $m$  fading parameters with  $m_i = 2$ . Fig. 8 plots the exact SER with 4QAM for  $Q = 2$  and  $N = 3$ . The case of  $\rho = 0$  represents orthogonal codes. We see a

reduction in the SER as  $\rho$  increases. We also see that the diversity order is not affected by cross correlation. As such, the nonorthogonal codes which permit broader applications can be used for higher throughput without sacrificing the error rate significantly.

## V. CONCLUSIONS

In this paper, we analyzed the SER of STNC in a distributed cooperative network where  $L$  sources communicate with a single destination with the assistance of  $Q$  relays. For  $M$ -PSK and  $M$ -QAM modulation, new exact closed-form expressions of SER over independent but not necessarily identically distributed Nakagami- $m$  fading channels were derived. Moreover, the asymptotic SER was derived to reveal the network performance in the high SNR regime. Specifically, the asymptotic SER reveals that the diversity order of STNC was determined by the Nakagami- $m$  fading parameters of all the channels. Simulation results were used to validate our analytical expressions and to examine the impact of Nakagami- $m$  fading parameters, relay location, power allocation, and nonorthogonal codes on the SER.

## APPENDIX A

### PROOF OF (20)

According to Fig. 9, all poles are located in a closed curve. According to the residue theorem, the integral over a closed curve can be expressed as the linear combination of the residues of the poles in the curve. Mathematically, we have

$$\int_R^{-R} g(u)du + \int_{C_R} g(z) dz = 2\pi j \sum_{k=0}^N \text{Res}[g(z_k), z_k], \quad (42)$$

where  $C_R$  is the counterclockwise semicircular curve in Fig. 3. The absolute value of  $\int_{C_R} g(z) dz$  in (42) can be upper bounded as

$$\begin{aligned} \left| \int_{C_R} g(z) dz \right| &\leq \int_{C_R} |g(z)| dz \\ &= \int_{C_R} \left| \left( \prod_{n=0}^N \left( 1 - \frac{jza_n}{m_n} \right)^{-m_n} \right) e^{-jzv} \right| dz \\ &\leq \int_{C_R} \left| \prod_{n=0}^N \frac{1}{(1 - ja_n z)^{m_n}} \right| |e^{-jzv}| dz \end{aligned}$$



$$= \int_{C_R} \prod_{n=0}^N \left| \frac{1}{(1 - ja_n z)^{m_n}} \right| dz. \quad (43)$$

When  $R \rightarrow \infty$ , which indicates that the integral range of  $g(u)$  is from  $\infty$  to  $-\infty$ , we find the property of (43) as

$$\begin{aligned} \left| \int_{C_R} g(z) dz \right| &= \int_{C_R} \prod_{n=0}^N \frac{1}{a_n^{m_n} |z|^{m_n} + O(z^{m_n})} dz \\ &= \left( \prod_{n=0}^N \frac{1}{a_n^{m_n}} \right) \int_{C_R} \frac{1}{|z|^{\sum_{n=0}^N m_n}} dz \\ &= \left( \prod_{n=0}^N \frac{1}{a_n^{m_n}} \right) \frac{\pi}{R^{\sum_{n=0}^N m_n - 1}} \\ &\rightarrow 0. \end{aligned} \quad (44)$$

Substituting (44) into (42), we obtain (20) and thus complete this proof.

#### REFERENCES

- [1] A. Sendonaris, E. Erkip, , and B. Aazhang, "User cooperation diversity—Part I and Part II," *IEEE Trans. Commun.*, vol. 51, no. 11, pp. 1927–1948, Nov. 2003.
- [2] J. N. Laneman, D. N. C. Tse, and G. W. Wornell, "Cooperative diversity in wireless networks: Efficient protocols and outage behavior," *IEEE Trans. Inf. Theory*, vol. 50, no. 12, pp. 3062–3080, Dec. 2004.
- [3] P. L. Yeoh, M. Elkashlan, Z. Chen, and I. B. Collings, "SER of multiple amplify-and-forward relays with selection diversity," *IEEE Trans. Commun.*, vol. 59, no. 8, pp. 2078–2083, Aug. 2011.
- [4] N. Yang, M. Elkashlan, and J. Yuan, "Outage probability of multiuser relay networks in Nakagami- $m$  fading channels," *IEEE Trans. Veh. Technol.*, vol. 59, no. 5, pp. 2120–2132, Jun. 2010.
- [5] R. Ahlswede, N. Cai, S.-Y. R. Li, and R. W. Yeung, "Network information flow," *IEEE Trans. Inform. Theory*, vol. 46, no. 4, pp. 1204–1216, Jul. 2000.
- [6] S.-Y. R. Li, , R. W. Yeung, and N. Cai, "Linear network coding," *IEEE Trans. Inform. Theory*, vol. 49, no. 2, pp. 371–381, Feb. 2003.
- [7] J. Li, J. Yuan, R. Malaney, M. Xiao, and W. Chen, "Full-diversity binary frame-wise network coding for multiple-source multiple-relay networks over slow-fading channels," *IEEE Trans. Veh. Technol.*, vol. 61, no. 3, pp. 1346–1360, Mar. 2012.
- [8] M. Xiao and T. Aulin, "Optimal decoding and performance analysis of a noisy channel network with network coding," *IEEE Trans. Commun.*, vol. 57, no. 5, pp. 1402–1412, May 2009.
- [9] M. Xiao and M. Skoglund, "Multiple-user cooperative communications based on linear network coding," *IEEE Trans. Commun.*, vol. 58, no. 12, pp. 3345–3351, Dec. 2010.
- [10] J. Li, J. Yuan, R. Malaney, M. H. Azmi, and M. Xiao, "Network coded LDPC code design for a multi-source relaying system," *IEEE Trans. Wireless Commun.*, vol. 10, no. 5, pp. 1538–1551, May 2011.

- [11] J. Du, M. Xiao, and M. Skoglund, "Cooperative network coding strategies for wireless relay networks with backhaul," *IEEE Trans. Commun.*, vol. 59, no. 9, pp. 2502–2514, Sep. 2011.
- [12] J. Yuan, Z. Chen, B. Vucetic, and W. Firmanto, "Performance and design of space-time coding in fading channels," *IEEE Trans. Commun.*, vol. 51, no. 12, pp. 1991–1996, Dec. 2003.
- [13] E. G. Larsson and W.-H. Wong, "Nonuniform unitary space-time codes for layered source coding," *IEEE Trans. Wireless Commun.*, vol. 3, no. 3, pp. 958–965, May 2004.
- [14] D. Wang, X. Gao, and X. You, "Low complexity turbo receiver for multi-user STBC block transmission systems," *IEEE Trans. Wireless Commun.*, vol. 5, no. 10, pp. 2625–2632, Oct. 2006.
- [15] J. Yuan, Z. Chen, Y. Li, and L. Chu, "Distributed space-time trellis codes for a cooperative system," *IEEE Trans. Wireless Commun.*, vol. 8, no. 10, pp. 4897–4905, Oct. 2009.
- [16] R. H. Y. Louie, Y. Li, H. A. Suraweera, and B. Vucetic, "Performance analysis of beamforming in two-hop amplify and forward relay networks with antenna correlation," *IEEE Trans. Wireless Commun.*, vol. 8, no. 6, pp. 3132–3141, Jun. 2009.
- [17] P. L. Yeoh, M. Elkashlan, and I. B. Collings, "MIMO relaying: Distributed TAS/MRC in Nakagami- $m$  fading," *IEEE Trans. Commun.*, vol. 59, no. 10, pp. 2678–2682, Oct. 2011.
- [18] J. N. Laneman and G. W. Wornell, "Distributed space-time coded protocols for exploiting cooperative diversity in wireless networks," *IEEE Trans. Inf. Theory*, vol. 49, no. 10, pp. 2415–2425, Oct. 2003.
- [19] Y. Jing and B. Hassibi, "Distributed space-time coding in wireless relay networks," *IEEE Trans. Wireless Commun.*, vol. 5, no. 12, pp. 3524–3536, Dec. 2006.
- [20] Y. Jing and H. Jafarkhani, "Distributed differential space-time coding for wireless relay networks," *IEEE Trans. Commun.*, vol. 56, no. 7, pp. 1092–1100, Jul. 2008.
- [21] Y. Jing, "Combination of MRC and distributed space-time coding in networks with multiple-antenna relays," *IEEE Trans. Wireless Commun.*, vol. 9, no. 8, pp. 2550–2559, Aug. 2010.
- [22] W. Wang, S. Jin, X. Gao, K.-K. Wong, and M. R. McKay, "Power allocation strategies for distributed space-time codes in two-way relay networks," *IEEE Trans. Signal Process.*, vol. 58, no. 10, pp. 5331–5339, Oct. 2010.
- [23] H.-Q. Lai and K. J. R. Liu, "Space-time network coding," *IEEE Trans. Signal Process.*, vol. 59, no. 4, pp. 1706–1718, Apr. 2011.
- [24] Y. Yang, H. Hu, J. Xu, and G. Mao, "Relay technologies for WiMAX and LTE-advanced mobile systems," *IEEE Commun. Mag.*, vol. 47, no. 10, pp. 100–105, Oct. 2009.
- [25] M. Nakagami, "The  $m$ -distribution: A general formula of intensity distribution of rapid fading," *Statistical Methods in Radio Wave Propagation*, vol. 40, pp. 757–768, Nov. 1962.
- [26] I. S. Gradshteyn and I. M. Ryzhik, *Table of Integrals, Series, and Products, 7th ed.* Academic Press, New York, 2007.
- [27] L. Ahlfors, *Complex Analysis.* McGraw-Hill, New York, 1953.
- [28] M. K. Simon and M.-S. Alouini, *Digital Communication over Fading Channels - A Unified Approach to Performance Analysis.* Wiley-Interscience, 2000.
- [29] D. Tse and P. Viswanath, *Fundamentals of Wireless Communication.* Cambridge University Press, 2005.

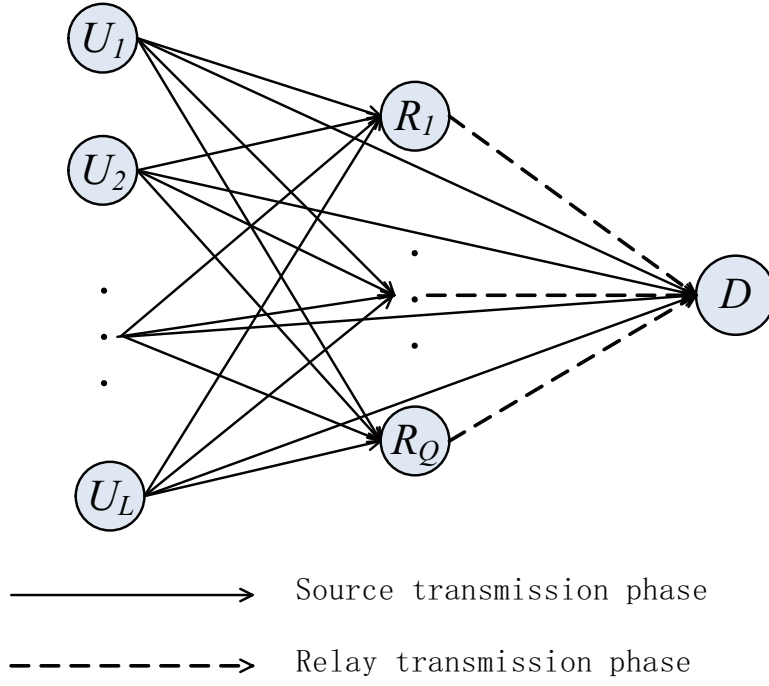


Fig. 1. System model.

	$T_1$	$\cdots$	$T_l$	$\cdots$	$T_L$		$T_{L+1}$	$\cdots$	$T_{L+q}$	$\cdots$	$T_{L+Q}$
$U_1$	$x_1$	$\cdots$	$0$	$\cdots$	$0$	$R_1$	$f_1(x)$	$\cdots$	$0$	$\cdots$	$0$
$\vdots$	$\vdots$	$\ddots$	$\vdots$	$\cdots$	$\vdots$	$\vdots$	$\vdots$	$\ddots$	$\vdots$	$\cdots$	$\vdots$
$U_l$	$0$	$\cdots$	$x_l$	$\cdots$	$0$	$R_q$	$0$	$\cdots$	$f_q(x)$	$\cdots$	$0$
$\vdots$	$\vdots$	$\cdots$	$\vdots$	$\ddots$	$\vdots$	$\vdots$	$\vdots$	$\cdots$	$\vdots$	$\ddots$	$\vdots$
$U_L$	$0$	$\cdots$	$0$	$\cdots$	$x_L$	$R_Q$	$0$	$\cdots$	$0$	$\cdots$	$f_Q(x)$
	Source transmission phase						Relay transmission phase				

Fig. 2. A framework of space-time network coding.

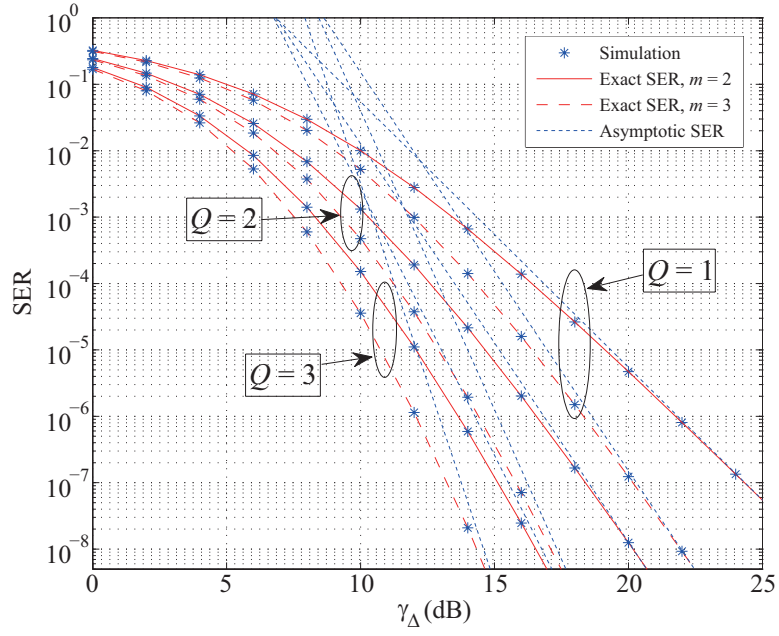


Fig. 3. Exact and asymptotic SER with 4QAM for  $Q = 1, 2, 3$ ,  $c_{(i+1)l} = c_{i+1} = c_i + 0.1\gamma_{\Delta}$ , and  $c_0 = c_{0l} = 0.6\gamma_{\Delta}$ .

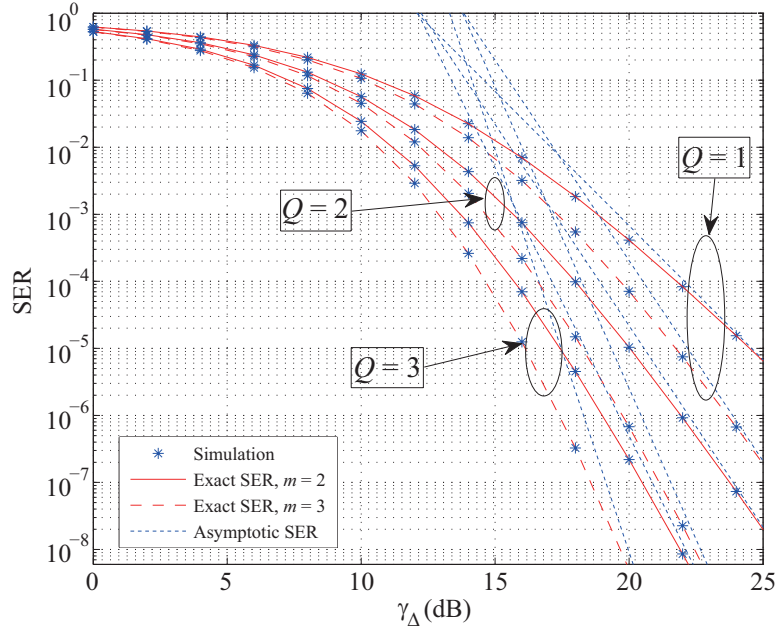


Fig. 4. Exact and asymptotic SER with 8PSK for  $Q = 1, 2, 3$ ,  $c_{(i+1)l} = c_{i+1} = c_i + 0.1\gamma_{\Delta}$ , and  $c_0 = c_{0l} = 0.6\gamma_{\Delta}$ .

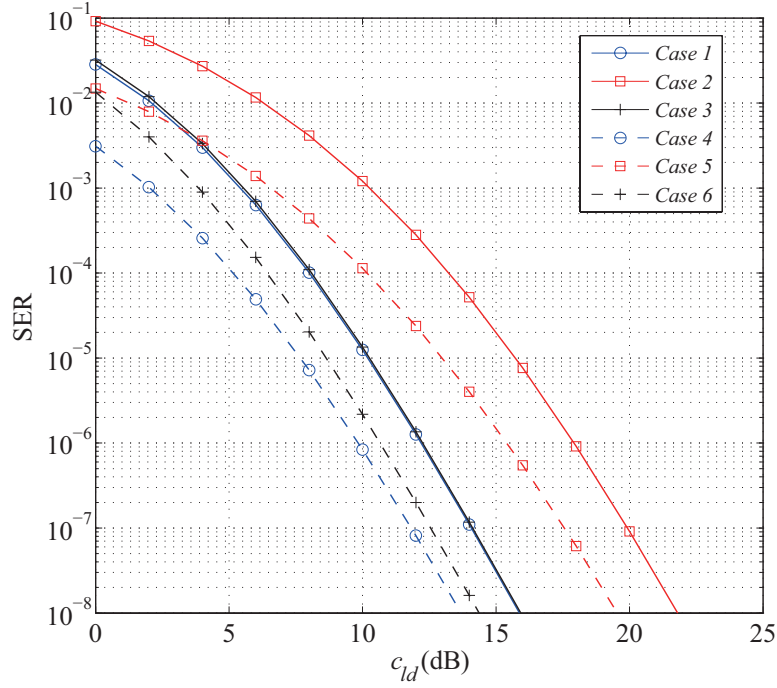


Fig. 5. Exact SER with BPSK for  $Q = 2$ ,  $m = 2$  and 6 cases: *Case 1*:  $d_{l1} = 0.2, d_{l2} = 0.3, d_{1d} = 1.1, d_{2d} = 1.2$ ; *Case 2*:  $d_{l1} = 0.2, d_{l2} = 0.3, d_{1d} = 2, d_{2d} = 2.2$ ; *Case 3*:  $d_{l1} = 0.8, d_{l2} = 0.9, d_{1d} = 1.1, d_{2d} = 1.2$ ; *Case 4*:  $d_{l1} = 1.1, d_{l2} = 1.2, d_{1d} = 0.2, d_{2d} = 0.3$ ; *Case 5*:  $d_{l1} = 2, d_{l2} = 2.2, d_{1d} = 0.2, d_{2d} = 0.3$ ; and *Case 6*:  $d_{l1} = 1.1, d_{l2} = 1.2, d_{1d} = 0.8, d_{2d} = 0.9$ .

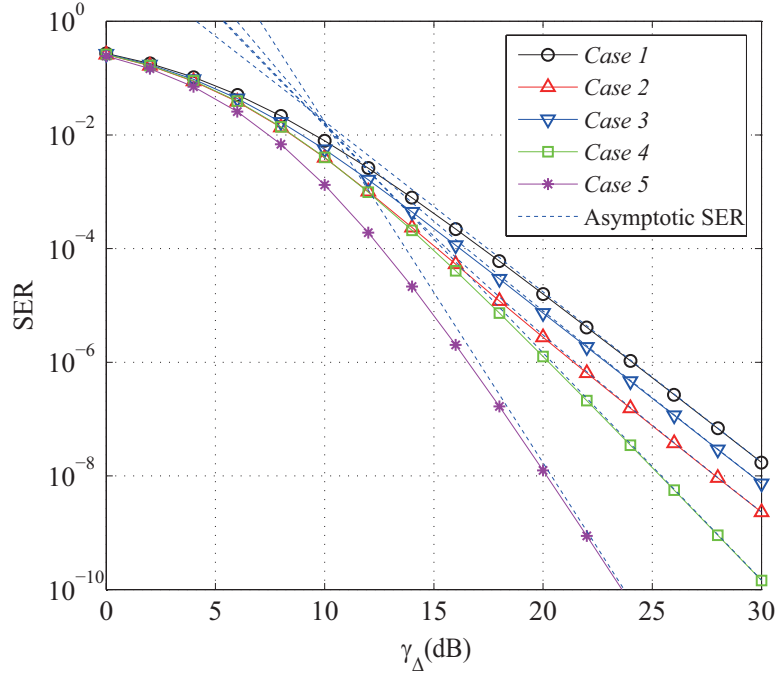


Fig. 6. Exact SER with 4QAM for  $Q = 2$ ,  $c_{(i+1)l} = c_{i+1} = c_i + 0.1\gamma_{\Delta}$ ,  $c_0 = c_{0l} = 0.6\gamma_{\Delta}$  and 6 cases: *Case 1*:  $m_i = m = 1$ ; *Case 2*:  $m_{l1} = 1, m_{l2} = 1, m_{1d} = 1, m_{1d} = 2, m_{2d} = 2$ ; *Case 3*:  $m_{l1} = 2, m_{l2} = 2, m_{1d} = 1, m_{1d} = 1, m_{2d} = 1$ ; *Case 4*:  $m_{l1} = 1, m_{l2} = 2, m_{1d} = 1, m_{1d} = 1, m_{2d} = 2$ ; *Case 5*:  $m_i = m = 2$ .

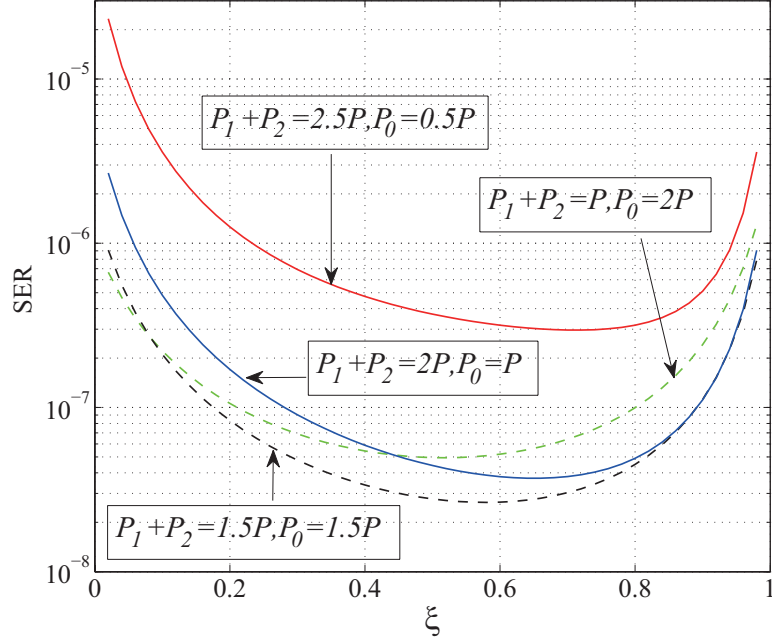


Fig. 7. Exact SER with 4QAM for  $Q = 2$ ,  $m = 2$  with  $d_{l1} = 0.8$ ,  $d_{l2} = 1$ ,  $d_{1d} = 0.9$ ,  $d_{2d} = 0.7$ , and different power allocation  $P_1, P_2, P_3$ .

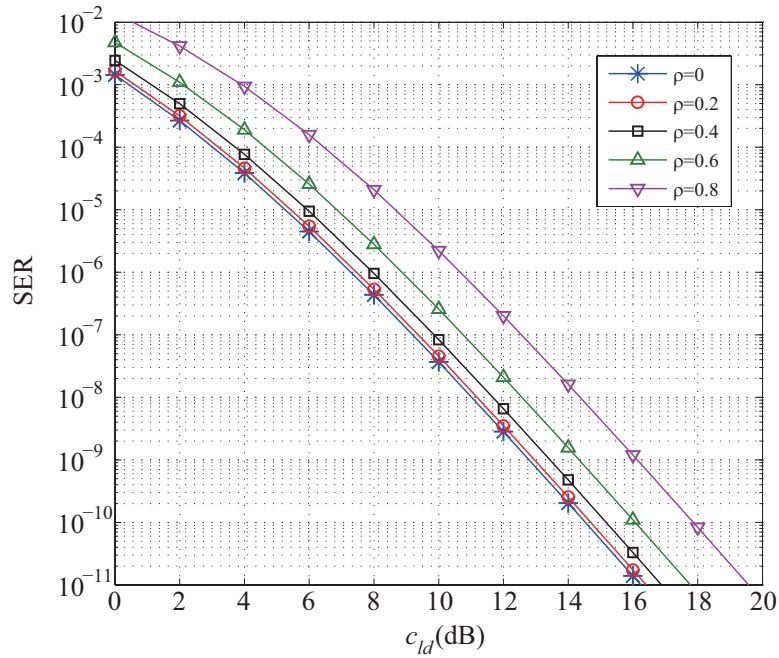


Fig. 8. Exact SER with 4QAM for  $Q = 2$ ,  $N = 3$ ,  $m_i = 2$  and different cross correlation  $\rho$  with  $d_{l1} = 0.6$ ,  $d_{l2} = 0.8$ ,  $d_{1d} = 0.6$  and  $d_{2d} = 0.8$ , where  $d_{ld}$  is normalized as  $d_{ld} = 1$ .

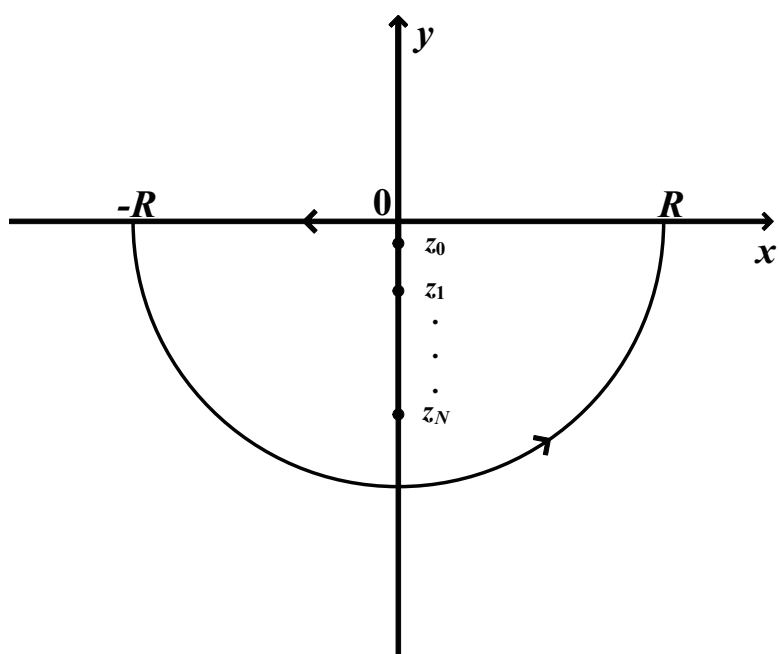


Fig. 9. The distribution of the poles.